



**HAL**  
open science

# Delta RCS Expression of Linear Time-Variant Transponders based on Polarization Modulation

Nicolas Barbot

► **To cite this version:**

Nicolas Barbot. Delta RCS Expression of Linear Time-Variant Transponders based on Polarization Modulation. 2022 IEEE 12th International Conference on RFID Technology and Applications (RFID-TA), Sep 2022, Cagliari, Italy. pp.55-58, 10.1109/RFID-TA54958.2022.9923962 . hal-04009071

**HAL Id: hal-04009071**

**<https://hal.science/hal-04009071>**

Submitted on 28 Feb 2023

**HAL** is a multi-disciplinary open access archive for the deposit and dissemination of scientific research documents, whether they are published or not. The documents may come from teaching and research institutions in France or abroad, or from public or private research centers.

L'archive ouverte pluridisciplinaire **HAL**, est destinée au dépôt et à la diffusion de documents scientifiques de niveau recherche, publiés ou non, émanant des établissements d'enseignement et de recherche français ou étrangers, des laboratoires publics ou privés.

# Delta RCS Expression of Linear Time-Variant Transponders based on Polarization Modulation

Nicolas Barbot

Univ. Grenoble Alpes, Grenoble INP, LCIS,

F-26000 Valence, France.

nicolas.barbot@lcis.grenoble-inp.fr

**Abstract**—This paper investigates the maximum read range which can be achieved by linear time-variant chipless sensor based on polarization modulation. Analytical expression of the differential RCS is derived as a function of the polarization scattering parameters of the transponder. Expressions are valid for all scatterers and allow to determine the maximum read range considering polarization modulation. From the derived expressions, a linear time-variant sensor based on a dipole array is designed to maximize the read range. Simulation and measurement confirm the approach and achieve a read range of 20 m in real environment. This read range can outperform by a factor of 50 the one classically obtained with chipless RFID.

**Index Terms**—Linear Time-Invariant (LTI) system, Radar Cross-Section (RCS), Radio Frequency Identification (RFID).

## I. INTRODUCTION

Linear Time-Variant (LTV) transponders are a recent paradigm allowing one to drastically increase the read range compared to classical Linear Time-Invariant (LTI) chipless sensors. The principle relies on the modulation of the power backscattered by the tag. This modulated power can be detected by the reader at a distance higher than 10 m.

The modulation of the reflected power appears very early in the literature [1], unfortunately this principle has never been investigated by the chipless community which only focuses on LTI systems with associated read range of few dozens of centimeters [2]. Note that the vast majority of chipless tags presented in the literature are LTI systems. For all LTI systems (which include classical chipless tags and all stationary objects present in the environment), the received signal can be obtained by realizing the convolution between the transmitted signal of the reader and the impulse response of the tag (or the object). On the other side, LTV transponders violates the time-invariance property and are able to modulate their reflected/backscattered signal. These transponders cannot be described by an impulse response (or a transfer function).

Modulation realized by scatterers can rely on different principles. Load modulation [1], in which the impedance connected to an antenna is modified as a function of time is, by far, the most popular approach. This principle has been the foundation of the Ultra High Frequency (UHF) RFID technology [3]. However different types of modulation can also be used and do not require the presence of a chip. In [4], the author uses a mechanical load modulation to backscatter a 32 bits message to the reader at a distance of 2 m with a transmitted power of only 5 dBm. In [5], authors use the

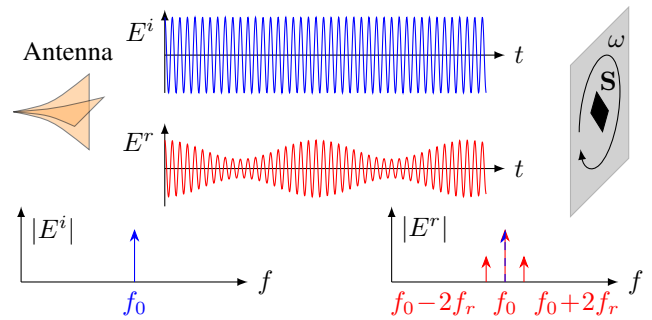


Fig. 1. Principle of the proposed method based on rotating scatterer. Transmitted signal in blue, received signal in red.

polarization variations generated by a rotating patch in the normal incidence and achieve a read range of 13 m. In [6], [7], authors investigate the Doppler modulation with different dipoles and reach a reading distance of 15 m.

LTV transponders (which gathers any scatterer whose response is a function of time) and LTI transponders (*i.e.*, chipless tags) can actually be seen as two opposite technologies. Moreover, the former one benefits from interesting properties compared to the classical chipless technology. First, these transponders can be read using a simple Continuous Wave (CW) signal which significantly reduces the reader complexity compared to chipless readers based on Ultra-Wideband (UWB) signals. Second, LTV transponders can also be read with a single measurement which simplifies the reading procedure compared to chipless systems where a second measurement in the same environment without the tag is required. Moreover, LTV transponders are also characterized by a non zero delta RCS which is proportional to the modulated power backscattered by the tag (whereas delta RCS associated to a chipless tag is equal to zero since the LTI tags can not modulate the backscattered signal). Finally and more importantly, read range associated to LTV tags can be increased with the transmitted power and can reach more than 10 m [1], [5], [7]. Note that this high read range can only be achieved by breaking the time-invariance property. This can be simply done by rotating or translating the scatterer. If this condition is not satisfied (*i.e.*, if the scatterer is motionless), it can be fully described by a LTI system and the associated read range cannot be increased with the transmitted

power and is bound by few dozens of centimeters [2].

While the performance of LTV scatterer can already outperform by a factor 30 the read range associated to the chipless technology, the maximum read range which can be achieved is still unknown. This paper investigates the maximum read range which can be achieved using a polarization modulation. For this, analytical expressions for the delta RCS are derived and allow to determine the maximum read range of the proposed system. Simulations and measurements confirm the approach which achieves a read range of 35 m and 25 m in free-space and real environment respectively while satisfying regulation standards.

## II. RESULTS

### A. Model

The relation between the complex envelope in time of reflected electric field  $\mathbf{E}^r$  by a scatterer impinged by an the incident field  $\mathbf{E}^i$  can be described by its polarization scattering matrix  $\mathbf{S}$  as:

$$\begin{bmatrix} E_v^r \\ E_h^r \end{bmatrix} = \begin{bmatrix} S_{vv} & S_{vh} \\ S_{hv} & S_{hh} \end{bmatrix} \cdot \begin{bmatrix} E_v^i \\ E_h^i \end{bmatrix} \quad (1)$$

where we can see the backscattered power is linear as a function of the incident power.

In [5], authors show that if any scatterer is rotating at a constant speed  $\omega = 2\pi f_r$  in a plane perpendicular the propagation vector, the backscattered field, in all polarizations can be expressed by (2) where we can see that the rotation generates two peaks at  $f_0 \pm 2f_r$  (see also red peaks in Fig. 1). Note that the presented model is valid for any scatterer. On the following, we consider in this study four different resonators: a C-shaped tag, a rectangular loop, a half-wavelength dipole without ground plane, and the proposed design based on a dipole array (see Fig. 2). Note that the two first scatterers are very selective and are classically used by the chipless technology. The third scatterer is a simple dipole without ground plane. The last design is based on an array of two half-wavelength dipoles spaced by a distance of  $\lambda/2$  allowing to maximize the read range. This design will be discussed in the next subsections. Finally, all resonators are rotated using a simple motor.

### B. Delta RCS

The modulated power which can be detected by the reader can be linked to the differential RCS  $\sigma_d$  associated to the rotating scatterer. Differential RCS has been initially introduced in [8] to characterize the modulated power

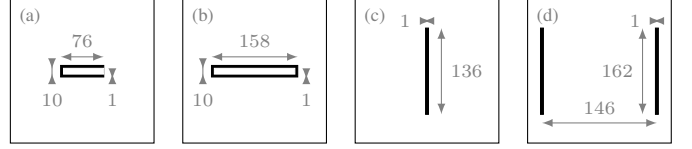


Fig. 2. Resonators used in the study: (a) C-shape, (b) rectangular loop, (c) dipole and the proposed design. All dimensions in millimeters.

backscattered by UHF tags. However, this definition has been generalized to any modulated tags in [9] based on a frequency domain definition.

Analytical expressions for the delta RCS can directly be extracted from (2) by determining the power associated to the sidebands for each polarization [5]. The following derivations are done for the vertical co-polarization, but the same method can be applied for the other polarizations. Results for all polarizations are presented at the end of the subsection.

From (2a), the dynamical power associated to components located at  $f_0 \pm 2f_r$  (i.e., the two red peaks in Fig. 1) can be linked to the differential RCS of the rotating tag by:

$$\sigma_{dvv} = 4\pi \left[ \left| \frac{S_{vv} - S_{hh} - 2jS_{vh}}{4} \right|^2 + \left| \frac{S_{vv} - S_{hh} + 2jS_{vh}}{4} \right|^2 \right] \quad (3)$$

By noting that the magnitude of the sum of 2 complex numbers  $z_1$  and  $z_2$  can be expressed as:  $|z_1 + z_2|^2 = |z_1|^2 + |z_2|^2 + |z_1| \cdot |z_2| \cos(\phi_1 - \phi_2)$ , with  $\phi_1$  and  $\phi_2$ , their respective phase, (3) can be rewritten as:

$$\sigma_{dvv} = 4\pi \left[ \frac{|S_{vv} - S_{hh}|^2 + 4|S_{vh}|^2}{8} + \frac{2|S_{vv} - S_{hh}| \cdot |S_{vh}| [\cos(\Delta\phi + \frac{\pi}{2}) + \cos(\Delta\phi - \frac{\pi}{2})]}{8} \right] \quad (4)$$

where  $\Delta\phi = \phi_{vv-hh} - \phi_{vh}$ . By developing the cosine functions, one can easily recognize that the second term is null. Finally, delta RCS associated to the rotating scatterer is equal to:

$$\sigma_{dvv} = 4\pi \frac{|S_{vv} - S_{hh}|^2 + 4|S_{vh}|^2}{8} = \sigma_{dhh} = \sigma_{dvh} \quad (5)$$

Note that this delta RCS is the same in all the polarizations.

Fig. 3 presents the delta RCS estimated in simulation and measurement for the presented scatterers. Each scatterer length has been optimized to maximize the delta RCS at 915 MHz (see Fig. 2). Simulations has been obtained using NEC2 which is based on the Method of Moments. This method is more

$$\begin{cases} S_{vv}(f) = \frac{S_{vv} + S_{hh}}{2} \delta(f - f_0) + \frac{S_{vv} - S_{hh} - 2jS_{vh}}{4} \delta(f - f_0 - 2f_r) + \frac{S_{vv} - S_{hh} + 2jS_{vh}}{4} \delta(f - f_0 + 2f_r) & (2a) \\ S_{hh}(f) = \frac{S_{vv} + S_{hh}}{2} \delta(f - f_0) + \frac{S_{hh} - S_{vv} + 2jS_{vh}}{4} \delta(f - f_0 - 2f_r) + \frac{S_{hh} - S_{vv} - 2jS_{vh}}{4} \delta(f - f_0 + 2f_r) & (2b) \\ S_{vh}(f) = \frac{2S_{vh} - j(S_{hh} - S_{vv})}{2} \delta(f - f_0 - 2f_r) + \frac{2S_{vh} + j(S_{hh} - S_{vv})}{2} \delta(f - f_0 + 2f_r) & (2c) \end{cases}$$

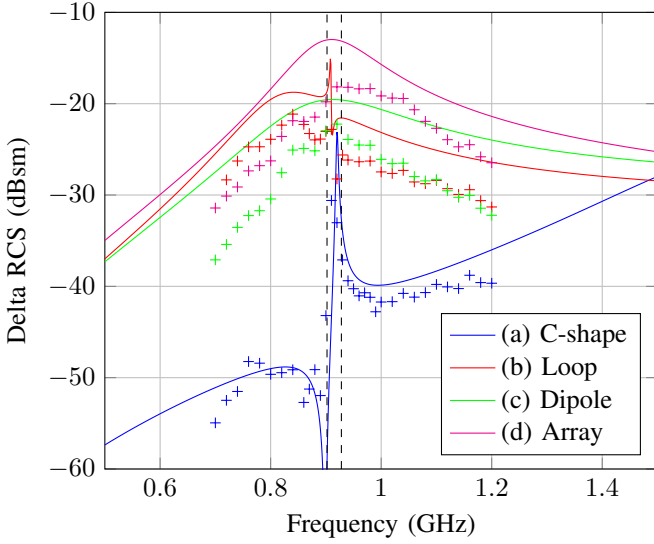


Fig. 3. Differential RCS of the proposed resonators. Simulation in plain lines. Measurement in anechoic chamber with marks.

accurate than FDTD for determining the backscattered field amplitude from highly resonating structures. Simulated delta RCS is directly based on (5) in which  $S_{vv}$  (and  $S_{hv}$ ) and  $S_{hh}$  (and  $S_{hv}$ ) are determined by two simulations. Measurement bench uses a bistatic configuration placed in anechoic chamber. Measured delta RCS is estimated from the spectrum of the backscattered signal  $S_R(f - f_0)$  acquired with a spectrum analyzer (without empty measurement) and the following formula [9]:

$$\sigma_d = \frac{(4\pi)^3 d_1^2 d_2^2}{P_t G_t G_r \lambda^2} \times \left[ \int_{f_0-b}^{f_0-\epsilon} S_R(f - f_0) df + \int_{f_0+\epsilon}^{f_0+b} S_R(f - f_0) df \right] \quad (6)$$

Spectrum analyzer span is set to  $2b = 1$  kHz around  $f_0$ . Static contribution (due to leakage and reflections) is removed over a bandwidth of  $2\epsilon = 125$  Hz.

Differential RCS obtained in simulation and measurement are in good agreement, the same difference of 5 dB is observed between simulated and measured delta RCS for all the scatterers and corresponds to the cumulative attenuation, loss and mismatch in the setup (*i.e.*, cables, connectors, antennas...) which are not taken into account in (6). Note that the proposed approach based on an array of two dipoles separated by a distance of  $\lambda/2$  allows to maximize the delta RCS compared to all the other structures while keeping a compact surface of  $\lambda^2/4$ . The maximum value of  $\sigma_d$  for the array achieves  $-13$  dBsm at 915 MHz which is 6 dB higher than a simple dipole and 2 dB higher than a loop resonator.

### C. Read Range

When the tag is rotating, read range in real environments (*i.e.*, non-isolated channels) could be derived from a modified

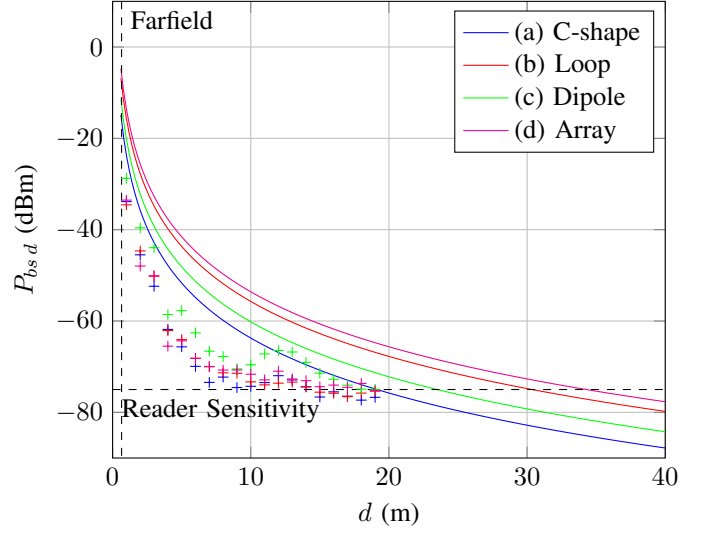


Fig. 4. Modulated power as a function of the distance between the reader and the tag. Simulated delta RCS considering free space propagation (see (7)) in plain lines. Measurement in outdoor environment with marks.

from of the radar equation [2]:

$$d_{LTV} \leq \sqrt[4]{\frac{P_t G_t G_r \lambda^2 \sigma_d}{(4\pi)^3 P_{rr \min}}} \quad (7)$$

where  $P_t$  and  $P_{rr \min} = 2N_0 b$  are the transmitted power and the receiving reader sensitivity respectively (*i.e.*, the minimal differential backscattered power which can be detected by the reader).

Results are presented in Fig. 4 for simulated and measured read range. For both cases, frequency has been chosen at the exact resonant frequency of each scatterer. Effective Isotropic Radiated Power (EIRP) is set to 4 W considering antennas of gain  $G_t = G_r = 6$  dBi. For simulation results,  $\sigma_d$  is extracted from Fig. 3. For measurement results, the setup is placed in outdoor environment, a power amplifier is used to reach the maximum EIRP and the backscattered power  $P_{bs,d}$  is measured (without empty measurement) as a function of the distance between the reader and the scatterer.

Note that the measured modulated power  $P_{bs,d}$  is a decreasing function of the distance and then remains constant due to the noise floor associated to the setup (which was measured at  $-75$  dBm, when no scatterer was rotating). Read range for the different scatterers can directly be extracted from Fig. 4 in free space and real environment. In free space, distance higher than 20 m can be obtained for all the scatterers. In real environment, read range is reduced compared to free space mainly due to the reflection with the ground, misalignments and the different attenuation and losses associated to the setup but remains higher than 10 m for all scatterers. Finally, the proposed design achieves the highest read range measured at 20 m. Note that classical LTI chipless tags can not operate at distances higher than 40 cm [2]. Thus, the proposed LTV design outperforms the read range associated to the chipless RFID by a factor higher than 50.

### III. CONCLUSION

The paper presents a LTV chipless sensor based on polarization modulation which can be detected at long range. Analytical expression is derived as a function of the polarization scattering parameters. This expression allows to optimize the scatterer design to maximize the read range up to 20 m in real environment. and outperforms the one associated to classical chipless sensor by a factor higher than 50.

### REFERENCES

- [1] H. Stockman, "Communication by means of reflected power," *Proceedings of the IRE*, vol. 36, no. 10, pp. 1196–1204, Oct. 1948.
- [2] N. Barbot, O. Rance, and E. Perret, "Classical RFID versus chipless RFID read range: Is linearity a friend or a foe?" *IEEE Trans. Microw. Theory Techn.*, vol. 69, no. 9, pp. 4199–4208, Sep. 2021.
- [3] K. Finkenzeller, *RFID handbook: fundamentals and applications in contactless smart cards, radio frequency identification and near-field communication*. John Wiley & sons, 2010.
- [4] M. S. Reynolds, "A 500°C tolerant ultra-high temperature 2.4 GHz 32 bit chipless RFID tag with a mechanical BPSK modulator," in *2017 IEEE International Conference on RFID (RFID)*, 2017, pp. 144–148.
- [5] N. Barbot and E. Perret, "Linear time-variant chipless RFID sensor," *IEEE RFID J.*, vol. 6, pp. 104–111, 2022.
- [6] A. Lazaro, M. Lazaro, R. Villarino, and P. De Paco, "New radar micro-Doppler tag for road safety based on the signature of rotating backscatters," *IEEE Sensors J.*, vol. 21, no. 6, pp. 8604–8612, Mar. 2021.
- [7] A. Azarfar, N. Barbot, and E. Perret, "Towards chipless RFID technology based on micro-doppler effect for long range applications," in *2021 IEEE MTT-S International Microwave Symposium (IMS)*, Atlanta, GA, Jun. 2021, pp. 819–822.
- [8] P. V. Nikitin, K. V. S. Rao, and R. D. Martinez, "Differential RCS of RFID tag," *Electron. Lett.*, vol. 43, no. 8, pp. 431–432, Apr. 2007.
- [9] N. Barbot, O. Rance, and E. Perret, "Differential RCS of modulated tag," *IEEE Trans. Antennas Propag.*, vol. 69, no. 9, pp. 6128–6133, Sep. 2021.